ISSN 2176-5480

22nd International Congress of Mechanical Engineering (COBEM 2013)
November 3-7, 2013, Ribeirão Preto, SP, Brazil

PROPOSAL OF CURVE FITTING FOR SHEAR STRESS DURING GEL BREAKING OF THIXOTROPIC DRILLING FLUIDS

Diogo E. V. Andrade[1]
Matheus Toneli Rodrigues[2]
Emanuel Vitor Ceccon[3]
Ana Cristine B. da Cruz[4]
Admilson T. Franco[5]
Cezar O. R. Negrão[6]
Thermal Science Laboratory (LACIT) Post-graduate Program in Mechanical and Materials Engineering (PPGEM), Federal University of Technology - Parana (UTFPR) – Av. Sete de Setembro, 3165, CEP 80.230-901 – Curitiba-PR-Brazil
[1]diogoandrade@utfpr.edu.br, [2]matheus_toneli@hotmail.com, [3]emanuel_evc8@hotmail.com, [4]anacrisbcruz@hotmail.com, [5]admilson@utfpr.edu.br, [6]negrao@utfpr.edu.br

Abstract*. Drilling fluids usually gels at rest in order to avoid cuttings to lie over the drill bit when circulation is interrupted. At flow start-ups, pumping pressure higher than the circulation pressure is necessary to exceed the gel strength. The gelation may have significant importance, specially, in deep waters where high pressures and low temperatures take place. In the current work, controlled shear rate and shear stress rheometric tests were conducted to investigate drilling fluid yielding. The results show that the gel yield stress depends not only on the shear rate but also on the shear strain. An algebraic constitutive equation that accounts for both shear rate and hystory is proposed to predict the gel yield stress. This equation is quite useful to model pressure peaks that take place during drilling fluid flow start-ups.*

Keywords*: drilling fluids; thixotropic; rheometric tests; yield stress; curve fitting.*

1. INTRODUCTION

Drilling fluids are usually formulated to build up a gel-like structure at rest in order to avoid cuttings precipitation at well bottom when circulation is discontinued. However, high pressures are required to break-up the gel and consequently, to resume circulation. These high pressures cannot exceed the formation fracture pressure so as to avoid damage to the wellbore walls, preventing loss of fluid circulation. A correct prediction for pressure within the wellbore during start-up is, therefore, important for appropriate drilling operations.

This reduction of strength whenever a fluid is sheared after rest and the recuperation of strength when stress is subsequently relieved is called thixotropy (Mewis and Wagner, 2009). In spite of the several works dedicated to model thixotropy (Barnes, 1997; Mewis and Wagner, 2009; Mujumdar *et al.*, 2002; Abu-Jdayil, 2003; Roussel *et al.*, 2004; Labanda *et al.*, 2004; Dullaert and Mewis, 2006; Armellin *et al.*, 2006; Owens, 2006; Roussel, 2006; Beris *et al.*, 2008; Jarny *et al.*, 2008; Mendes, 2009; Ardakani, 2011; Alexandrou *et al.*, 2013; Azikri de Deus and Dupim, 2013; Mendes and Thompson, 2013), the gel breaking phenomenon still lacks understanding. These models are not only complex to understand and solve but also dependent on several parameters that need to be fit to experimental data. In addition, rheometric tests have also been used to evaluate gel break-up at drilling fluid flow start-ups. For instance, controlled shear rate and stress tests have been performed to determine the material yield stress.

In the current work, a fitting curve is proposed in order to represent the shear stress as the material is yielded during gel breaking. The equation based on the solution of a second order ordinary differential equation depends on six parameters that are fitted to rheometric data.

2. EXPERIMENTAL SECTION

2.1. Materials and Methods

Rheometric tests were performed to two oil-based drilling fluids by using the Haake Mars III rotational rheometer, a 35 mm parallel plate sensor and 1.0 mm gap. The temperature was controlled by a Peltier-Thermostatic bath system. The minimum rheometer torque detected by the rheometer is 5.10^{-8} Nm.

As the material is thixotropic, the same shearing procedure was applied in order to assure repeatability to the tests and establish the same shear history to the sample. The procedure was as follows: (i) the sample is introduced into the rheometer; (ii) the sensor is placed in its test position; (iii) the sample is left aging for 10 min at the test temperature; (iv) a shear rate varying from 0 to 1000 s^{-1} in 10 seconds is imposed to the sample; (v) the 1000 s^{-1} constant shear rate is maintained for 5 minutes; (vi) the shear rate is reduced from 1000 to 0 s^{-1} in 10 seconds; (vii) the sample is left aging for five more minutes and finally; (viii) the test is initiated.

Controlled stress and shear rate tests were then conducted in order to evaluate the material yield stress.

2.2. Controlled shear rate tests

These tests were performed by varying the shear rate from zero to a final value in 10 seconds and then, this final value is maintained for 10 more minutes. Five final shear rate values were applied: 5, 10, 20, 30, 40, and 50 s^{-1}. Figure 1.a shows the shear stress as function of logarithmic time scale for the five controlled shear rate tests. As can be seen, the shear stress rises up to a maximum value and then falls. The region of increasing stress corresponds to a predominantly elastic behavior of the material and the maximum is the stress necessary to yield the material, named as critical stress, τ_c, in the current work. Note that the higher the final shear rate, the higher the magnitude of the maximum and the earlier the maximum takes place. It is worth noting that the peaks occur within the first second of test, in other words, before the shear rate reaches its final value. After gel breaking, the material shows predominantly viscous response. When the shear rate reaches its final value at 5 seconds, the shear stress depicts a small peak. Finally, the stress is reduced tending to the equilibrium.

The shear stress as a function of strain for the five tests is shown in Fig. 1.b. As shown by the red dotted line, the critical stress takes place at almost constant critical strain, in this case, 0.45. In other words, the critical strain is shear rate independent and seems to be a material property within this range of applied shear rate.

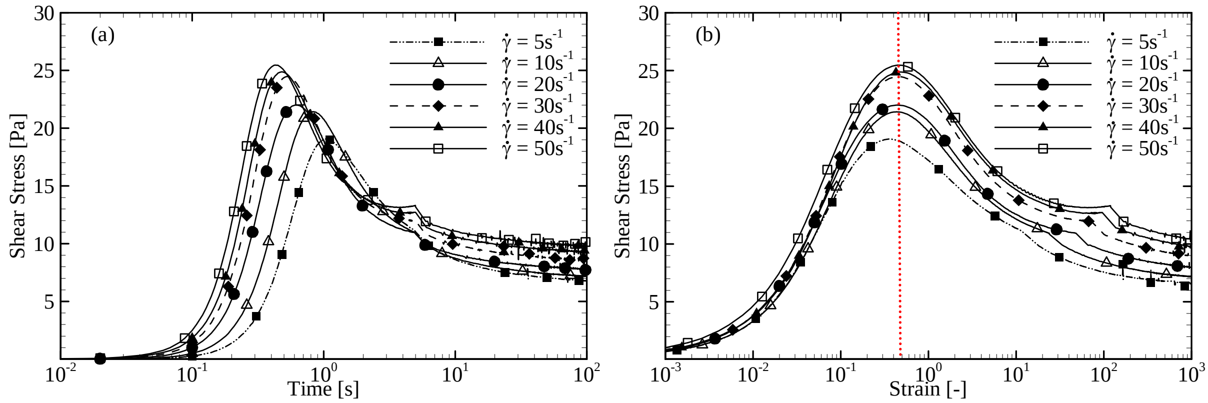

Figure 1. Shear stress as a function of (a) time and (b) strain for controlled shear rates tests performed at 25ºC.

2.3. Controlled shear stress tests

In this section, the results obtained from controlled stress tests are presented. A constant shear stress was imposed to the sample and the strain was measured as a function of time. Small strains are noted in the predominantly elastic region and the gel is broken when the strain increases abruptly. On the other hand, if the applied stress is smaller than the material yield stress, the material deforms within the elastic region and the strain stabilizes afterwards.

Considering the order of magnitude of 20 Pa obtained for critical stress in the controlled strain tests, five different values of shear stress, 1, 3, 6, 8, and 12 Pa, were imposed in order to determine the minimal stress that can break the gel structure. Figure 2 presents the time variation of strain for the five controlled stress tests. At the test start-up for a stress of 12Pa, the strain changes smoothly up to approximately 0.2 seconds when the gel is broken and the material undergoes large deformations. It is noteworthy that the 12 Pa stress is smaller than the range of critical stress observed in the controlled shear rate tests (see Fig. 2).

Figure 2 also shows that the gel breaks for smaller stresses and that the smaller the stress the higher is the gel breaking time. For instance, the gel breaks-up after three hours for a constant shear stress of 1 Pa. As proposed by Barnes and Walters (1985), the material does not present a constant yield stress as it flows after a long time for a quite small applied stress. As also noted, the gel structure took place at almost the same critical strain of 0.7.

3. CURVE FITTING

An equation is now proposed to describe gel breaking for controlled shear rate tests. The equation aims at representing the variation of shear stress as a function of strain as shown in Fig. 1.b.

For the results obtained in the equilibrium, the shear stress shown in Fig. 1.b can be well represented by the Bingham fluid equation (Bingham, 1916):

$$\tau(\infty) = \tau_{y,\infty} + \eta\dot{\gamma} \tag{1}$$

where τ , $\tau_{y,\infty}$ and η are , respectively, the shear stress, equilibrium yield stress and the plastic viscosity.

ISSN 2176-5480

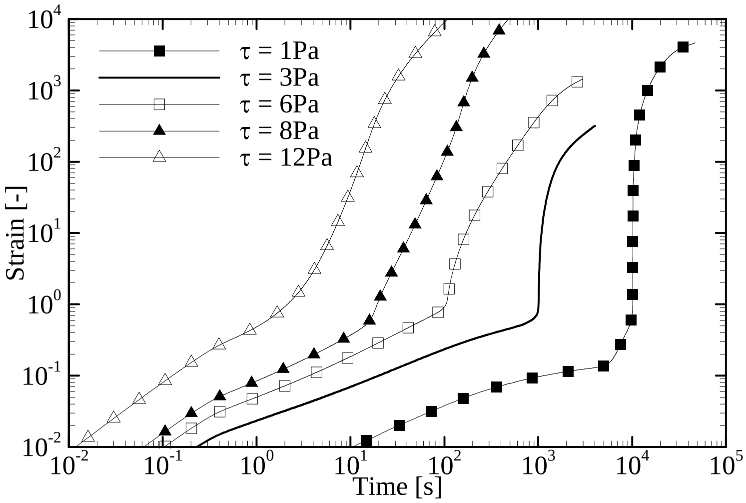

Figure 2. Shear strain as a function of time for controlled stress tests performed at 25ºC.

A Bingham-based equation is then proposed to represent the results of Fig. 1.b:

$$\tau = \tau_y + \eta\dot{\gamma} \tag{2}$$

Figure 3 shows the values of τ_y as computed by using the results of Fig. 1.b and Eq. (2) (i.e., $\tau_y = \tau - \eta\dot{\gamma}$). As can be seen, τ_y is a function of not only shear rate, $\dot{\gamma}$, but also strain, γ. In addition, τ_y is zero for not strained material and tends to an equilibrium value, $\tau_{y,\infty}$, for highly strained material.

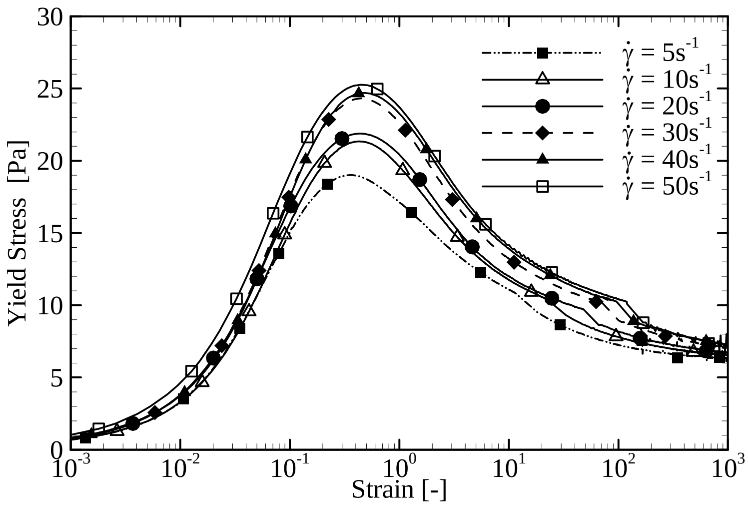

Figure 3. Variation of τ_y as a function of strain for the five tests described in section 3.

By analyzing the results of Fig. 3, one can see that each curve can be well described by a second order differential equation as follows,

$$\frac{d^2\tau_y}{d\gamma^2} + a\frac{d\tau_y}{d\gamma} + b(\tau_y - \tau_{y,\infty}) = 0 \tag{3}$$

where *a* and *b* are fitting parameters of the equation. It is worth mentioning that this equation is proposed as a fitting curve rather than a physical model. However, equation can be quite useful to predict the material yielding in practical applications. The solution of Eq. (3) for $\lambda^2 = a^2 - 4b > 0$ is given by:

$$\tau_y(\dot{\gamma},\gamma) = \tau_{y,\infty} + e^{-\frac{1}{2}a\gamma}\left(C_1 e^{\frac{1}{2}\lambda\gamma} + C_2 e^{-\frac{1}{2}\lambda\gamma}\right) \tag{4}$$

where C_1 and C_2 depends on the problem boundary conditions that are defined as τ_y =0 for γ =0 and $\tau_y = \tau_{y,c}$ for $\gamma = \gamma_c$. $\tau_{y,c}$ is the maximum value of τ_y that takes place at the critical strain, γ_c. As noted, this equation complies with

ISSN 2176-5480

the physical behavior shown in Fig. 1 as the yielding is a function of strain and the maximum stress, a function of shear rate. The higher the shear rate the higher the critical stress.

By using these boundary conditions, the values of C_1 and C_2 are obtained:

$$C_1 = -\left[\frac{\left(\tau_{y,c} - \tau_{y,\infty}\right)e^{\frac{1}{2}a\gamma_c} + \tau_{y,\infty}e^{-\frac{1}{2}\lambda\gamma_c}}{e^{-\frac{1}{2}\lambda\gamma_c} - e^{\frac{1}{2}\lambda\gamma_c}}\right] \tag{5}$$

$$C_2 = \frac{\left(\tau_{y,c} - \tau_{y,\infty}\right)e^{\frac{1}{2}a\gamma_c} + \tau_{y,\infty}e^{\frac{1}{2}\lambda\gamma_c}}{e^{-\frac{1}{2}\lambda\gamma_c} - e^{\frac{1}{2}\lambda\gamma_c}} \tag{6}$$

Nevertheless, as shown in Fig. 3, $\tau_{y,c}$ depends on the magnitude of shear rate. The following equation is then proposed to be fit to the measured results:

$$\tau_{y,c} = A\dot{\gamma}^B \tag{7}$$

where A and B are also fitting parameters.

Therefore, the proposed formulation has only six parameters to be fit to experimental data. This number of parameters is comparatively small in comparison to other thixotropy models available in the literature and can be easily obtained from shear rate controlled tests.

4. RESULTS

As already mentioned, the set of proposed equations have six parameters that need to be fit to controlled shear rate test results. Two of them, the plastic viscosity and $\tau_{y,\infty}$, are obtained from equilibrium shear stress data and *A* and *B* are determined from the values of $\tau_{y,c}$. The two remaining parameters, *a* and *b*, are fit to the complete set of values of Fig. 3. The least square method was used to fit all the parameters.

The proposed equations were then fit to two set of rheometric data available for two different drilling fluids. The set of results shown in the above figures is for the fluid named as A, whereas the results for Fluid B were obtained from Negrão *et al.* (2011). Both fluids A and B are oil based drilling fluids with different components concentration. The fitting data for both fluids are depicted in Tab. 1.

Comparison between measured and computed values for fluids A and B are illustrated, respectively, in Figs. 4 and 5. As can be seen, because of the composition of the materials, the Fluid A gel strength (analyzed by the critical stress, τ_c) is higher than the gel strength of Fluid B. The differences between the experimental and computed values evaluated at the peak ($\Delta\tau_y$) and at the equilibrium ($\Delta\tau_\infty$) are shown in Tab. 2. As shown, the computed values are quite close to the measured data for both fluids mainly in the elastic region. However, the proposed formulation deviates slightly from the measured values after gel breaking because the formulation is unable to represent the still existing elastic component of the stress observed in the measured values after gel breaking. Finally, the results are quite close in the equilibrium.

Table 1: Fitting parameters for Fluids A and B.

Parameter	Fluid A	Fluid B
η [Pa.s]	0.0637	0.0993
$\tau_{y,\infty}$ [Pa]	6.2647	3.582
A [Pa.s^B]	15.746	6.042
B [-]	0.1217	0.1544
a [-]	10.16	10.48
b [-]	1.796	2.186

ISSN 2176-5480

Table 2: Differences between measured and computed values for Fluids and A and B.

Shear rate	Fluid A		Fluid B	
	$\Delta\tau_\infty$ [%]	$\Delta\tau_c$ [%]	$\Delta\tau_\infty$ [%]	$\Delta\tau_c$ [%]
$5\,s^{-1}$	0.9	0.8	5.0	1.2
$10\,s^{-1}$	0.3	-2.3	-4.2	-1.3
$20\,s^{-1}$	0.2	3.6	0.4	0.1
$30\,s^{-1}$	-1.0	-2.1	-2.0	-1.3
$40\,s^{-1}$	-0.8	-0.2	0.2	-1.0
$50\,s^{-1}$	1.1	0.3	1.1	0.6

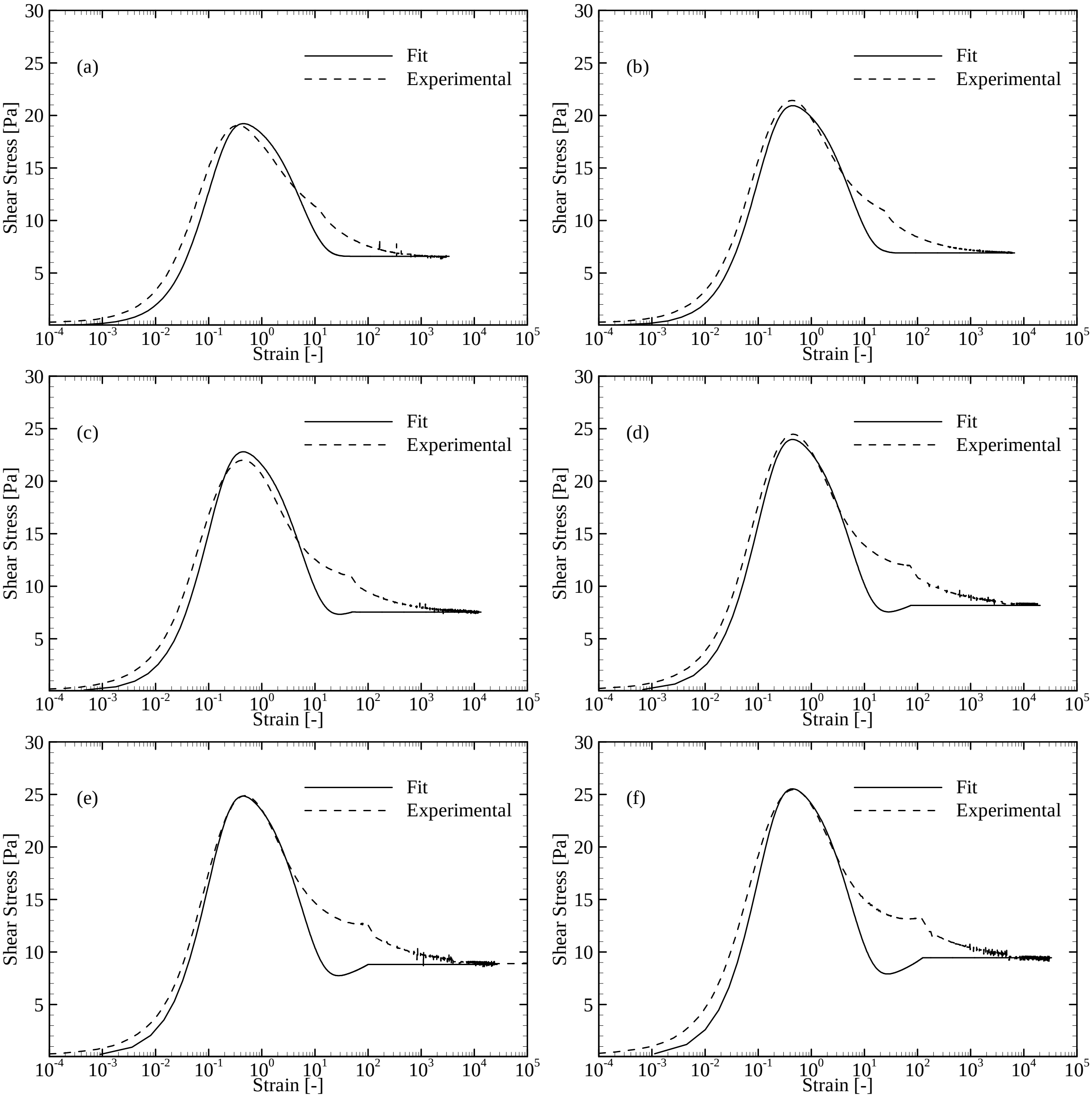

Figure 4. Comparison between measured and computed shear stresses for different shear rates obtained for Fluid A: (a) $5\,s^{-1}$; (b) $10\,s^{-1}$; (c) $20\,s^{-1}$; (d) $30\,s^{-1}$; (e) $40\,s^{-1}$; (f) $50\,s^{-1}$.

ISSN 2176-5480

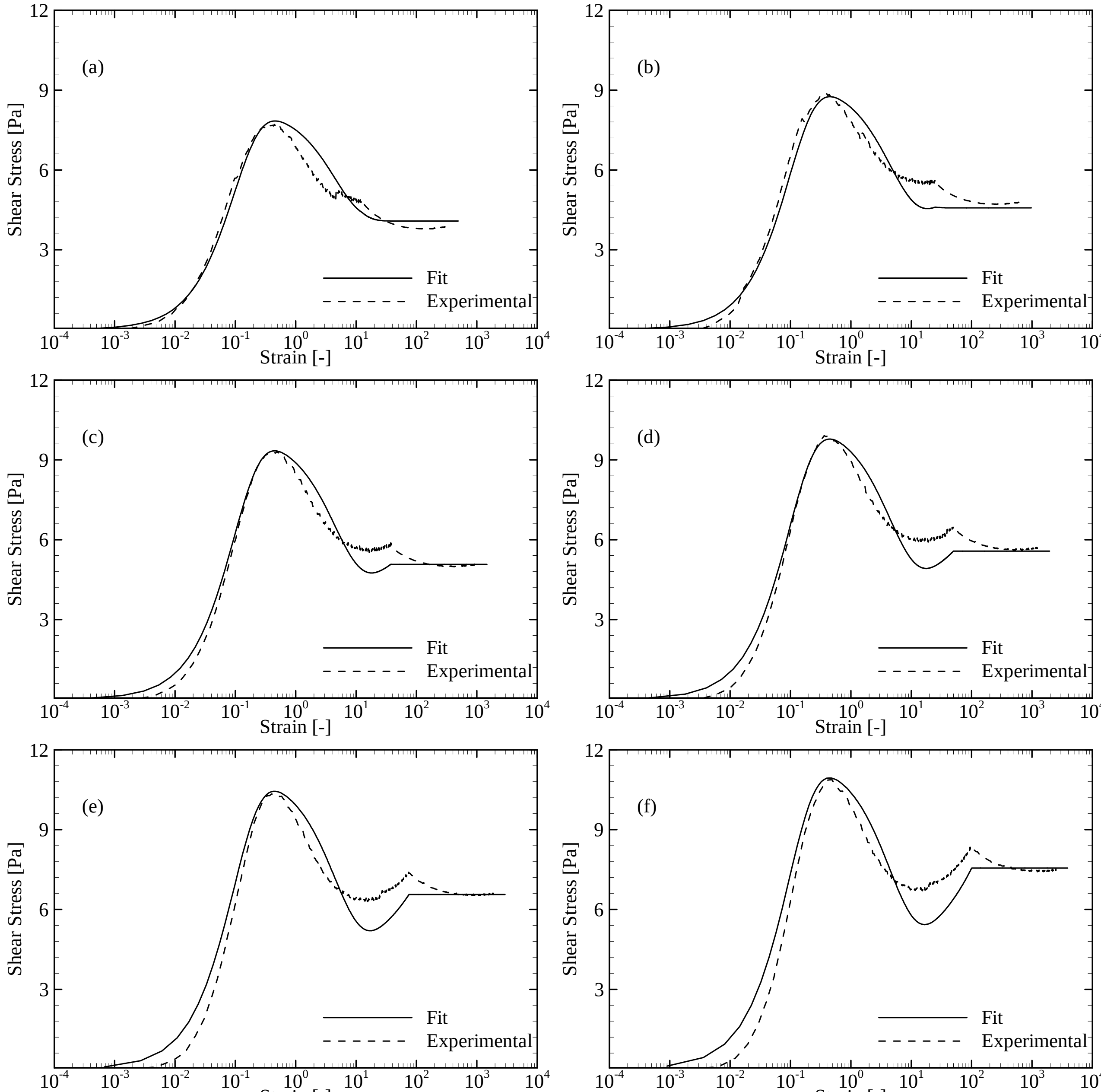

Figure 5. Comparison between measured and computed shear stresses for different shear rates obtained for Fluid B: (a) 5 s^{-1}; (b) 10 s^{-1}; (c) 15 s^{-1}; (d) 20 s^{-1}; (e) 30 s^{-1}; (f) 40 s^{-1}.

5. CONCLUSIONS

Gel breaking of drilling fluids is analyzed in the current work. Rheometric tests obtained by controlling shear rate shows that the maximum shear stress (the critical value) takes place at approximately same strain independently of the applied shear rate. In shear stress controlled tests, the gel is yielded even for quite small values of stress. Nevertheless, the smaller the applied shear stress, the longer is the yielding time. Similarly to controlled shear rate tests, gel breaking took place at almost the same strain. Despite the critical value of strain being different for controlled shear rate and controlled shear stress tests, both values seem to be a material dependent property.

Finally, a set of equations was proposed to predict gel breaking for controlled shear rate tests. It is worth noting that the set of equations comply with the physical behavior of gel breaking as the yielding is a function of strain and the maximum stress is a function of shear rate. This formulation requires a small number of fitting parameters that are easily obtained from the results of shear rate controlled tests. A comparison between measured and computed stress values for two different fluids was performed. The proposed equation fits quite well to the region of predominantly

ISSN 2176-5480

elastic behavior of the material. In addition, the differences between the maximum and the equilibrium measured and computed values lie with an error band of 5%.

6. ACKNOWLEDGEMENTS

The authors acknowledges the financial support of PETROBRAS S/A, ANP (Brazilian National Oil Agency) and CNPq (The Brazilian National Council for Scientific and Technological Development).

7. REFERENCES

Abu-Jdayil, B., Modelling the time-dependent rheological behavior of semisolid foodstuffs, *J. Food Eng.*, 57, 97-102, 2003.
Alexandrou, A., N., Florides, G.C., Georgiou, G.C., Squeeze flow of semi-solid slurries, *J. Non-Newton. Fluid Mech.*, 193, 103–115, 2013.
Ardakani, H.A., Mitsoulis, E., Hatzikiriakos, S.G., Thixotropic flow of toothpaste through extrusion dies, *J. Non-Newton. Fluid Mech.*, 166, 1262–11271, 2011.
Armelin, E., Martí, M., Rudé, E., Laba0nda, J., Llorens, J., Alemán, C., A simple model to describe the thixotropic behavior of paints, *Prog.Org. Coatings*, 57, 229-235, 2006.
Azikri de Deus, H.P., Dupim, G.S.P., On behavior of the thixotropic fluids, *Physics Letters A*, 377, 478-485, 2013.
Barnes, H.A, Thixotropy – a review, *J. Non-Newton. Fluid Mech.*, 70, 1-33, 1997.
Barnes, H.A, Walters, K., The yield stress myth?, *Rheologica Acta*, 24, 323-326, 1985.
Bingham, E.C., An investigation of the laws of plastic flow, *U.S. Bureau of Standards Bulletin*, 13, 309-353, 1916.
Beris, A.N., Stiakakis, E., Vlassopoulos, D., A thermodynamically consistent model for the thixotropic behavior of concentrated star polymer suspensions, *J. Non-Newton. Fluid Mech.*, 152, 76–85, 2008.
Dullaert, K., Mewis, J., A structural kinetics model for thixotropy, *J. Non-Newton. Fluid Mech.*, 139, 21–30, 2006.
Jarny, S., Roussel, N., Le Roy, R., Coussot, P., Modelling thixotropic behavior of fresh cement pastes from MRI measurements, *Cement and Concrete Res.*, 38, 616-623, 2008.
Labanda, J., Marco, P., Llorens, J., Rheological model to predict the thixotropic behaviour of colloidal dispersions, *Colloids and Surfaces A: Physicochem. Eng. Aspects*, 249, 123-126, 2004.
Mendes, P.R.S., Modeling the thixotropic behavior of structured fluids, *J. Non-Newton. Fluid Mech.*, 164, 66-75, 2009.
Mendes, P.R.S., Thompson, R.L., A unified approach to model elasto-viscoplastic thixotropic yield-stress materials and apparent yield-stress fluids, *Rheologica Acta, v. online*, 1-17, 2013.
Mewis, J., Wagner, N.J., Thixotropy, *Adv. Colloid and Interface Sc.*, 147-148, 214-227, 2009
Negrão, C.O.R., Franco, A.T., Rocha, L.L.V., A weakly compressible flow model for the restart of thixotropic drilling fluids, *J. Non-Newton. Fluid Mech.*, 166, 1369-1381, 2011.
Mujumdar, A., Beris, A.N., Metzner, A.B., Transient phenomena in thixotropic systems, *J. Non-Newton. Fluid Mech.*, 102, 157–178, 2002.
Owens, R.G., A new microstructure-based constitutive model for human blood, *J. Non-Newton. Fluid Mech.*, 140, 57–70, 2006.
Roussel, N., Le Roy, R., Coussot, P., Thixotropy modelling at local and macroscopic scales, *J. Non-Newton. Fluid Mech.*, 117, 85–95, 2004.
Roussel, N., A thixotropy model for fresh fluid concretes: Theory, validation and applications, *Cement and Concrete Res.*, 36, 1797-1806, 2006.

8. RESPONSIBILITY NOTICE

The authors are the only responsible for the printed material included in this paper.